Nickel(II) Complexes of the Octaethyloxophlorin Dianion and Octaethyloxophlorin Radical Dianion†

Alan L. Balch,* Bruce C. Noll, Shane L. Phillips, Steven M. Reid, and Edward P. Zovinka

Department of Chemistry, University of California, Davis, California 95616

Received September 30, 1992®

The nickel(II) complex of the octaethyloxophlorin dianion, Ni^{II}(OEPOH), dissolves in pyridine to form red, air-sensitive solutions that contain diamagnetic, and therefore planar, four-coordinate Ni(II). Crystals of Ni^{II}(OEPOH) form from pyridine in the tetragonal space group $I4_1/a$ with a = 14.780(9) Å and c = 13.903(14) Å at 130 K with Z = 4. Refinement of 558 reflections and 102 parameters yielded R = 0.057 and R_w = 0.077. The complex is isomorphic with the tetragonal form of nickel(II) octaethylporphyrin. The meso hydroxyl groups are disordered over four equally populated sites, and the oxophlorin core shows a severely ruffled distortion. The Ni–N distance is 1.921(6) Å. Oxidation of Ni^{II}(OEPOH) in pyridine with dioxygen or diiodine yields brown solutions of the paramagnetic radical $(py)_2Ni$(OEPO•), which can be isolated in solid form and shows an isotropic EPR resonance at g = 2.006 in frozen pyridine at −90 °C. The magnetic moment of the radical in pyridine (2.5(2) μ_B) can be explained with strong antiferromagnetic coupling between the ligand radical and the nickel ion. Crystallization of the radical with exposure to air yields red parallelepipeds that form in the triclinic space group $P\bar{1}$ with a = 9.848(2) Å, b = 10.216(2) Å, c = 10.492(2) Å, α = 80.34(3)°, β = 89.82(3)°, γ = 66.36(3)° at 130 K with Z = 1. Refinement of 2318 reflections and 259 parameters yielded R = 0.036 and R_{w2} = 0.068. The nickel is six-coordinate, and the porphyrin is nearly planar. The Ni–N(oxophlorin) distances (2.062(2) and 2.063(2) Å) and the longer Ni–N(py) distance (2.226(2) Å) are indicative of the presence of high-spin (S = 1) Ni(II) in the solid. The meso oxygen is unequally disordered over four sites. Refinement of the oxygen atom occupancy led to the discovery that the solid contained additional oxygen above the one oxygen required for $(py)_2Ni^{II}$(OEPO•). Consequently, the crystals are formulated as containing both $(py)_2Ni^{II}$(OEPO•) and $(py)_2Ni^{II}$($OEPO_2$) where $OEPO_2$ represents a mixture of the *cis*- and *trans*-isomers of octaethyldioxoporphodimethene. In separate chemical experiments, the conversion of the nickel oxophlorin radical by dioxygen into a mixture of Ni^{II}(*cis*-$OEPO_2$) and Ni^{II}(*trans*-$OEPO_2$) has been confirmed.

Introduction

Meso-hydroxylation of a porphyrin produces a new class of macrocycle, the oxophlorins—**1**.[1] Oxophlorins have biological significance because they are believed to occur as initial

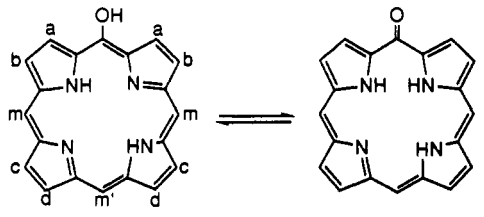

1a 1b

intermediates in the destruction of iron porphyrins by heme oxygenase.[2,3] While the oxophlorins can be considered as simple substituted porphyrins, they are much more readily oxidized than porphyrins.[4-6] Indeed, the ready formation of oxophlorin radicals has, at times, offered an impediment to the full characterization of oxophlorins and their metal complexes. In order to understand the formation, electronic structure, and reactivity of metal complexes of the oxophlorin macrocycle, we have undertaken first an examination of complexes of a totally redox-inactive metal (Zn^{II})[7] and now of a metal that is difficult to oxidize (Ni^{II}). In this context, it should be noted that oxidation of nickel(II) porphyrin complexes can lead to either metal or ligand oxidation (to form either $[PNi^{III}]^+$ or $[(P^•)Ni^{II}]$).[8-11]

This article is concerned with characterization of the nickel(II) complex of octaethyloxophlorin (**2**), Ni^{II}(OEPOH), and its oxidation in pyridine solution, which produces $(py)_2Ni$(OEPO•) (**3**). Oxidation of the oxophlorins in basic solution results in the removal of one electron and one proton from the macrocycle.

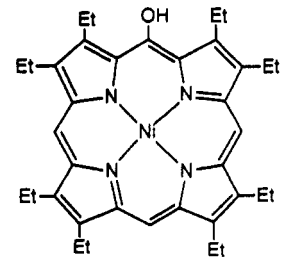

Ni^{II}(OEPOH)

2

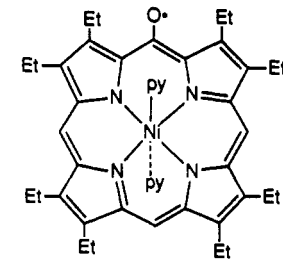

$(py)_2Ni^{II}$(OEPO•)

3

† Abbreviations: P, generic porphyrin dianion; OEP, dianion of octaethylporphyrin; OEP•, anion radical of octaethylporphyrin; OEPOH, dianion of octaethyloxophlorin; OEPO•, dianion radical of octaethyloxophlorin; TMPyP, dication of *meso*-tetrakis(*N*-methylpyridinium-4-yl)porphyrin; py, pyridine; Im, imidazole.

® Abstract published in *Advance ACS Abstracts*, October 1, 1993.

(1) Clezy, P. S. In *The Porphyrins*; Dolphin, D., Ed.; Academic Press: New York, 1978; Vol. II, p 103.
(2) O'Carra, P. In *Porphyrins and Metalloporphyrins*; Smith, K. M., Ed.; Elsevier: Amsterdam, 1976; p 123.
(3) Schmid, R.; McDonagh, A. F. In *The Porphyins*; Dolphin, D.; Ed.; Academic Press: New York, 1978; Vol. VI, p 257.
(4) Bonnett, R.; Dimsdale, M. J.; Sales, K. D. *J. Chem. Soc., Chem. Commun.* **1970**, 962.
(5) Fuhrop, J.-H.; Besecke, S.; Subramanian, J. *J Chem. Soc., Chem. Commun.* **1973**, 1.
(6) Fuhrop, J.-H.; Besecke, S.; Subramanian, J.; Mengerson, C.; Riesner, D. *J. Am. Chem. Soc.* **1975**, *97*, 7141.
(7) Balch, A. L.; Noll, B. C.; Zovinka, E. P. *J. Am. Chem. Soc.* **1992**, *114*, 3380.
(8) Wolberg, A.; Manassen, J. *Inorg. Chem.* **1970**, *9*, 2365.
(9) Dolphin, D.; Niem, T.; Felton, R. H.; Fujita, I. *J. Am. Chem. Soc.* **1975**, *97*, 5288.
(10) Johnson, E. C.; Niem, T.; Dolphin, D. *Can. J. Chem.* **1978**, *56*, 1381.
(11) Kim, D.; Miller, L. A.; Spiro, T. G. *Inorg. Chem.* **1986**, *25*, 2468.

0020-1669/93/1332-4730$04.00/0

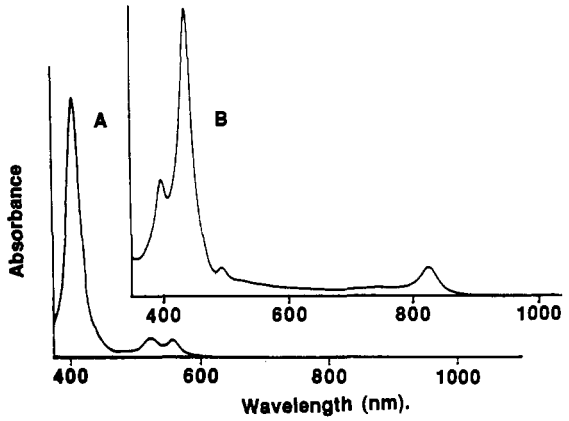

Figure 1. Electronic absorption spectra of pyridine solutions of (A) Ni^{II}(OEPOH) [λ_{max}, nm (ϵ, M^{-1} cm^{-1}): 408 (1.8 × 10^5), 523 (1.4 × 10^4), 556 (1.3 × 10^4)] and (B) $(py)_2Ni^{II}(OEPO^{\bullet})$ [λ_{max}, nm (ϵ, M^{-1} cm^{-1}): 398 (4.2 × 10^4), 438 (1.0 × 10^5), 492 (1.0 × 10^4), 742 (3.1 × 10^4), 825 (9.9 × 10^3)].

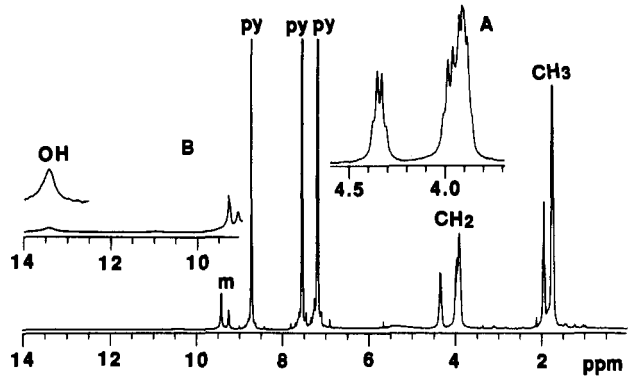

Figure 2. 300-MHz ^1H NMR spectrum of Ni^{II}(OEPOH) in pyridine-d_5 at 20 °C. Inset A shows an expansion of the methylene region. Inset B shows the OH resonance at 0 °C. Resonances originating from pyridine are noted as py.

Consequently, the oxidation products are neutral molecules, but their oxidation states correspond to the porphyrin π-cation radical species $[(P^{\bullet})Zn^{II}]^+$ or $[(P^{\bullet})Ni^{II}]^+$. The oxidation of Ni^{II}(OEPOH) to form a radical has been reported previously, and it was noted that the radical was in equilibrium with a dimer in chloroform solution.[6] Recently, this laboratory showed that crystallization of $(py)_2Ni^{II}(OEPO^{\bullet})$ from dichloromethane/ethanol produces the dimer **4** (as shown in eq 1) in which the two macrocycles are linked by a new carbon-carbon bond.[12]

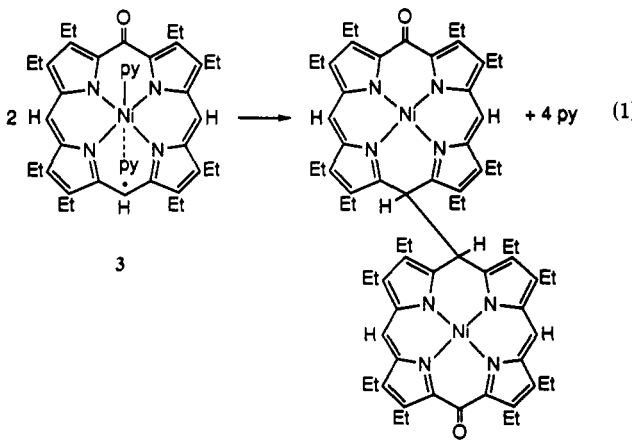

Results

Characterization of Ni^{II}(OEPOH) and $(py)_2Ni^{II}(OEPO^{\bullet})$. Red Ni^{II}(OEPOH) was prepared from H_2OEPOH by treatment with nickel acetate in a modification of a previous procedure.[6] We found that the nickel(II) complex was air stable under the acidic condition used for its preparation. However, solutions in basic solvents like pyridine were much more prone toward oxidation and needed to be carefully protected from dioxygen.

The electronic absorption spectrum of Ni^{II}(OEPOH) in pyridine solution is shown in trace A of Figure 1. This spectrum is similar to that of chloroform solutions reported earlier.[6] The similarity in these spectra indicates that the nickel complex retains its four-coordinate structure even in neat pyridine.

The presence of four-coordinate, planar nickel in these pyridine solutions is also manifest in the ^1H NMR spectrum. Figure 2 shows the spectrum of the complex in pyridine at 20 °C. The spectral pattern is that of a diamagnetic material. There are two meso resonances in a 2:1 intensity ratio at ca 9.4 ppm. The multiplets in the 3.8–4.5 ppm region are due to the methylene protons, and the features in the 1.7–2.0 ppm region are the methyl resonances. The methylene resonances appear as sets of four overlapping quartets. The appearance of the well-resolved, low-field quartet is particularly significant. This is readily assigned to the two methylene protons of the ethyl group closest to the meso hydroxyl group. The equivalence of the two methylene protons indicates that the two sides of the porphyrin plane are identical and rules out a diamagnetic five-coordinate structure. [Notice that for the analogous, five-coordinate (py)Zn(OEPOH··py) in pyridine, the fine structure of the methyl and methylene protons is not resolved.[7] Presumably this is due to rapid exchange of the axial pyridine ligand.] The hydroxyl proton appears as a broad resonance at ca. 13.5 ppm. When the sample is cooled to 0 °C, as shown in the inset, this narrows. A similar feature is seen in the ^1H NMR spectrum of (py)Zn(OEPOH··py).[7] Under similar conditions, solutions of Ni^{II}(OEP) in pyridine also show a ^1H NMR spectrum which is consistent with the presence of a diamagnetic, four-coordinate structure.

Solutions of Ni^{II}(OEPOH) in pyridine are very sensitive toward oxidation. Addition of diiodine or dioxygen results in the formation of brown solutions from which $(py)_2Ni(OEPO^{\bullet})$ can be isolated as red crystals. These redissolve in pyridine to give brown solutions. The absorption spectrum of $(py)_2Ni^{II}(OEPO^{\bullet})$ is shown in trace B of Figure 1. The low-energy feature at 825 nm is characteristic of the formation of the oxophlorin radical. For example, $(py)Zn^{II}(OEPO^{\bullet})$ shows a similar absorption at 819 nm.[7] Likewise, the formation of a broadened Soret peak with a shoulder at high energy is also seen in $(py)Zn^{II}(OEPO^{\bullet})$.[7] When $(py)_2Ni^{II}(OEPO^{\bullet})$ is dissolved in dichloromethane and crystallized by the slow addition of ethanol, red crystals of $[Ni_2(OEPO)_2]\cdot 2CH_2Cl_2$ are obtained. These have structure **4**.[12] Redissolution of these crystals in pyridine gives brown solutions with the electronic absorption spectrum shown in trace B of Figure 1.

In solution $(py)_2Ni^{II}(OEPO^{\bullet})$ is paramagnetic. The magnetic moment measured by the Evans technique is 2.5(2) μ_B at 20 °C, and it does not change on cooling over the temperature range +20 to −30 °C. The EPR spectrum in frozen pyridine solution at −90 °C consists of a signal at g = 2.006 (peak to peak width 25 G) with a very minor feature at g = 2.016 which may arise from an impurity.

The ^1H NMR spectrum of $(py)_2Ni^{II}(OEPO^{\bullet})$ in pyridine-d_5 shows three equally intense hyperfine-shifted resonances at 41.9, 22.0, and −12.4 ppm at 25 °C. These are probably due to the methylene protons, but the expected fourth resonance could not be detected nor could the meso resonances be observed.

Under prolonged exposure to dioxygen, pyridine solutions of $(py)_2Ni^{II}(OEPO^{\bullet})$ are slowly converted into a mixture in which Ni^{II}(*trans*-$OEPO_2$) (**5**) and Ni^{II}(*cis*-$OEPO_2$) (**6**) are present.

(12) Balch, A. L.; Noll, B. C.; Reid, S. M.; Zovinka, E. P. *J. Am. Chem. Soc.* **1993**, *115*, 2531.

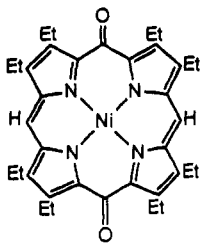

5 Ni^{II}(*trans*-$OEPO_2$)

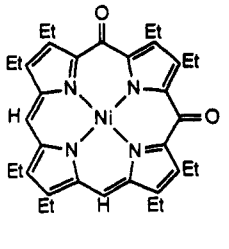

6 Ni^{II}(*cis*-$OEPO_2$)

These complexes have been independently prepared by metalation of *trans*- and *cis*-octaethyldioxoporphodimethene.[13] They have been separated and fully characterized both in the four-coordinate, diamagnetic forms and as six-coordinate, paramagnetic pyridine adducts.[13] The results of one experiment that demonstrates the conversion of **3** into these dioxo complexes are shown in Figure 3. In this experiment, a sample of **2** in pyridine was stored under a blanket of dioxygen for 3 days. The solution was evaporated, the residue was dissolved in chloroform, and the resultant solution was treated with aqueous sodium dithionite to reduce any of the nickel oxophlorin radical back to Ni^{II}(OEPOH). The chloroform solution was evaporated, and the residue was redissolved in chloroform-*d*. This solution produced the ^1H NMR spectrum shown in trace A of Figure 3. From the multiplicity of resonances, it is clear that several species are present. Trace B shows the spectrum of authentic Ni^{II}(*trans*-$OEPO_2$) (**5**) in chloroform. This allows a set of resonances in trace A to be identified with the presence of **5** in the oxygenated sample. The other resonances in trace A have also been identified by a spectral comparison with authentic samples of **2** and **6**.

In a similar experiment, a solution of Ni^{II}(OEPOH) in pyridine was stored under dioxygen for 3 days. The solution was evaporated, and the residue was redissolved. After the sample was separated by chromatography, a mixture of Ni^{II}(*trans*-$OEPO_2$) and Ni^{II}(*cis*-$OEPO_2$) was obtained in 80% isolated yield, and Ni^{II}(OEPOH) was recovered in 14% yield. In general, we have observed that chromatography on silica gel speeds up the formation of the dioxo products. Consequently, the yield of the dioxo products is larger in this experiment than in the one whose results are shown in Figure 3.

Crystal and Molecular Structure of Ni^{II}(OEPOH). The structure of this pyridine-free complex has been determined by X-ray crystallography. The complex is isomorphic with the tetragonal modification of Ni^{II}(OEP)[14] and has crystallographically imposed S_4 ($\bar{4}$) symmetry. The asymmetric unit consists of one-quarter of a nickel atom, one pyrrole ring with its ethyl substituents, and a meso carbon and its substituent (oxygen or hydrogen). Consequently, the meso oxygen is disordered. A view of the entire molecule with only one meso oxygen site drawn is shown in Figure 4. Atomic coordinates are given in Table I. Table II gives selected interatomic distances and angles.

The nickel ion is four-coordinate and planar. However, as with tetragonal Ni^{II}(OEP), the macrocycle is severely twisted into a ruffled shape. The out-of-plane displacements within the hydroxyporphin core are readily seen by turning to Figure 5, which shows a formal diagram for that core. The atom labels have been replaced by symbols that show the out-of-plane displacement of atoms in units of 0.01 Å. From this it is clear that the core of the meso-hydroxylated porphyrin is capable of undergoing the same sort of distortion from planarity as a porphyrin.

Because of the disorder, the C(5)–O distance 1.35(2) Å needs to be viewed with some caution. Nevertheless, its length, which is probably underestimated, is consistent with the presence of a meso hydroxyl rather than a ketonic substituent.

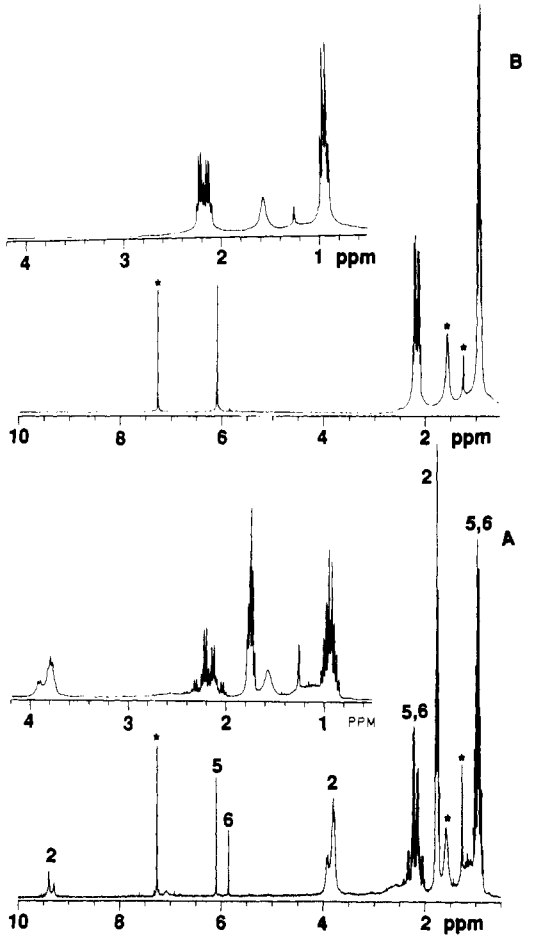

Figure 3. 300-MHz ^1H NMR spectra of (A) a dioxygen-treated sample of Ni^{II}(OEPOH) after removal of pyridine, reduction with sodium dithionite, and dissolution in chloroform-*d* (resonances of compounds **2**, **5**, and **6** labeled 2, 5, and 6, respectively and (B) a chloroform-*d* solution of Ni^{II}(*trans*-$OEPO_2$). Resonances are due to solvent impurities are labeled with an asterisk.

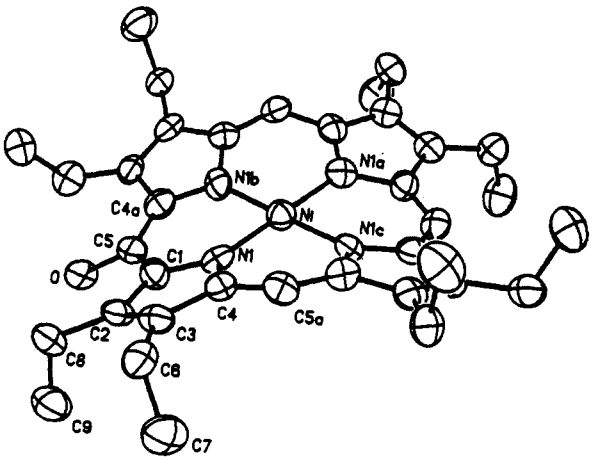

Figure 4. Perspective view of Ni^{II}(OEPOH) showing 50% thermal contours for all atoms. The location of only one meso oxygen substituent is shown.

The Ni–N distance (1.915(6) Å) is typical of that for four-coordinate nickel porphyrins and is close to the corresponding distance (1.929(3) Å) seen in the tetragonal modification of Ni^{II}(OEP).[14] The triclinic form of Ni^{II}(OEP) has a more nearly planar macrocycle and Ni–N distances of 1.959(2) and 1.957(2) Å.[15] In the nickel complex of 2,4-diacetyldeuteroporphyrin IX dimethyl ester, the Ni–N distances are 1.98, 1.95, 1.95, and 1.96 Å.[16]

(13) Balch, A. L.; Olmstead, M. M.; Phillips, S. L. *Inorg. Chem.* **1993**, *32*, 3931.
(14) Meyer, E. F., Jr. *Acta Crystallogr.* **1972**, *B28*, 2162.

Table I. Atomic Coordinates (×10⁴) and Equivalent Isotropic Displacement Coefficients (Å² × 10³) for Ni^{II}(OEPOH)

	x	*y*	*z*	U_{eq}
Ni	0	2500	6250	41.3(6)
O	2200(15)	409(12)	5394(16)	60(8)
N(1)	1294(4)	2563(4)	6246(4)	44(2)
C(1)	1897(5)	1864(5)	5984(5)	45(3)
C(2)	2822(5)	2187(6)	6045(4)	46(3)
C(3)	2789(5)	3034(5)	6378(5)	44(3)
C(4)	1848(5)	3278(5)	6477(5)	45(3)
C(5)	1625(5)	996(5)	5827(5)	44(3)
C(6)	3580(6)	3661(6)	6560(6)	58(3)
C(7)	3796(6)	4249(6)	5708(7)	71(4)
C(8)	3637(5)	1639(5)	5780(5)	50(3)
C(9)	3854(7)	1697(6)	4723(6)	74(4)

Table II. Bond Lengths (Å) and Angles (deg) for Ni^{II}(OEPOH)

Bond Lengths

Ni–N(1)	1.915(6)	C(4)–C(5a)	1.378(11)
N(1)–C(1)	1.412(10)	O–C(5)	1.356(22)
C(1)–C(2)	1.450(11)	N(1)–C(4)	1.375(10)
C(2)–C(3)	1.336(11)	C(1)–C(5)	1.362(11)
C(3)–C(4)	1.444(10)		

Bond Angles

N(1)–Ni–N(1a)	179.7(3)	N(1)–Ni–N(1b)	90.0(1)
Ni–N(1)–C(1)	126.6(5)	Ni–N(1)–C(4)	129.2(5)
C(1)–N(1)–C(4)	104.3(6)	N(1)–C(1)–C(2)	109.8(6)
N(1)–C(1)–C(5)	122.9(7)	C(2)–C(1)–C(5)	126.7(7)
C(1)–C(2)–C(3)	107.1(7)	C(2)–C(3)–C(4)	107.6(7)
N(1)–C(4)–C(3)	111.1(6)	N(1)–C(4)–C(5a)	121.6(7)
C(3)–C(4)–C(5a)	126.9(7)	O–C(5)–C(1)	119.3(10)
O–C(5)–C(4a)	114.9(11)	C(1)–C(5)–C(4a)	125.8(7)

Extensive attempts to grow ordered crystals of Ni^{II}(OEPOH) or to obtain crystals that correspond to the triclinic phase of Ni^{II}(OEP)[15] have not been fruitful.

Crystallization of $(py)_2Ni(OEPO^{\bullet})$. Crystals of this radical were obtained by diffusion of methanol into a pyridine solution of the radical without protection from atmospheric oxygen. This was done before, it was learned that the radical could be further oxidized to form **5** and **6**. The crystals that were obtained were isomorphic with those of $(py)_2Ni^{II}$(*trans*-$OEPO_2$) (**5**) and also $(py)_2Ni^{II}$(*cis*-$OEPO_2$) (**6**).[13] However, the structure of the crystals was solved and treated independently.

A view of the molecule is shown in Figure 6. Table III gives the atomic coordinates while Table IV presents selected bond distances and angles. The nickel ion sites at a center of symmetry, and the meso oxygen atoms are disordered. Two major sites that are related by a center of symmetry are present, along with two similarly related minor sites. Careful examination of the thermal parameters for these oxygen atoms revealed that the total oxygen occupancy was greater than 1. Refinement with the oxygen thermal parameter constrained to 0.0180 Å², a value just larger than the average thermal parameter of the carbon atoms of the porphyrin core, led to occupancies of 0.446 at the two major sites and 0.231 at the two minor sites. This leads to the apparent presence of 1.342 oxygen atoms per molecule. This anomally can readily be understood if the crystals actually contain a mixture of $(py)_2Ni(OEPO^{\bullet})$, $(py)_2Ni$(*trans*-$OEPO_2$), and its *cis*-isomer **6**. Thus the solid is formulated as $(py)_2Ni^{II}(OEPO^{\bullet})/(py)_2Ni^{II}(OEPO_2)$. The formation of these dioxo species is fully in accord with the observations on the reaction of $(py)_2Ni^{II}(OEOPO^{\bullet})$ with dioxygen that were described in a preceeding section. Moreover, those experiments were done only after the analysis of the crystallographic data suggested an anomalous occupancy of the meso oxygen sites.

Because these crystals contain a mixture of complexes, the individual bond parameters in Table IV represent average values

(15) Cullen, D. L.; Meyer, E. F., Jr. *J. Am. Chem. Soc.* **1974**, *96*, 2095.
(16) Hamor, T. A.; Caughey, W. S.; Hoard, J. L. *J. Am. Chem. Soc.* **1965**, *87*, 2305.

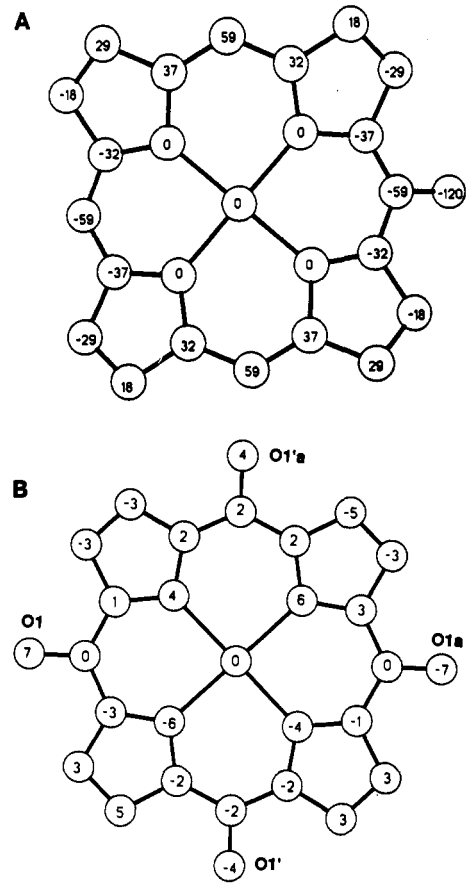

Figure 5. Diagrams of the oxophlorin cores for (A) Ni^{II}(OEPOH) and (B) $(py)_2Ni^{II}(OEPO^{\bullet})/(py)_2Ni^{II}(OEPO_2)$. Each atom label has been replaced by a number that represents the perpendicular displacement, in units of 0.01 Å, from the mean plane of the oxophlorin unit. Calculations of the coordinates of the core plane excluded the oxygen atoms.

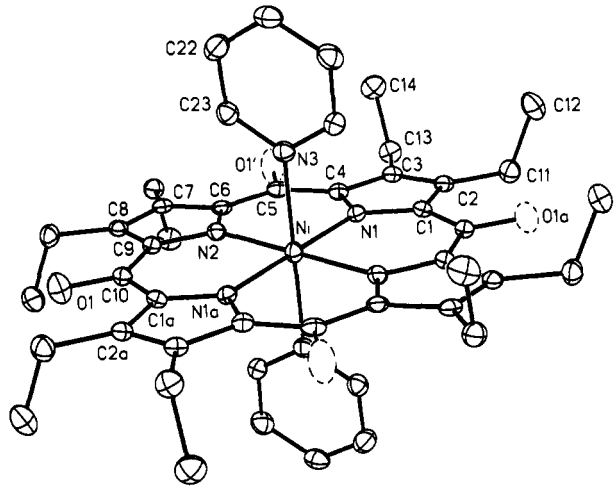

Figure 6. Perspective view of the molecule in $(py)_2Ni^{II}(OEPO^{\bullet})/(py)_2Ni^{II}(OEPO_2)$ showing 50% thermal contours for all atoms. The location of one of the meso oxygen positions (one of the two major forms with 0.44% site occupancy) is shown as a solid ellipse. The other major form has the oxygen attached to C(10a). The minor forms have oxygen attached to C(5) and C(5a), respectively. These are represented by dashed ellipses.

and must be viewed with caution. Nevertheless, it is certain that the nickel ion is six-coordinate with two axial pyridine ligands. The Ni–N(1) and Ni–N(2) distances (2.063(2)) and 2.062(2) Å) in the macrocyclic core are clearly longer than the Ni–N distance in Ni^{II}(OEPOH) and in the diamagnetic, four-coordinate nickel(II) porphyrins. These distances are also longer than those (1.945(9), 1.958(8), 1.944(9), 1.950(8) Å) in $\{Ni(OEP^{\bullet})ClO_4\}_2$.[17] However, they are close to the Ni–N distances (2.024(4), 2.052-

Table III. Atomic Coordinates ($\times 10^4$) and Equivalent Isotropic Displacement Coefficients ($Å^2 \times 10^3$) for $(py)_2Ni^{II}(OEPO^{\bullet})/(py)_2Ni^{II}(OEPO_2)$

	x	y	z	U_{eq}
Ni	5000	5000	5000	15(1)
N(1)	5641(2)	5538(2)	6638(2)	14(1)
N(2)	3346(2)	7064(2)	4499(2)	15(1)
N(3)	3448(2)	4226(2)	6104(2)	17(1)
O(1)	1363(5)	7488(5)	1488(4)	30(1)
O(1′)	3439(12)	9286(11)	6795(10)	49(3)
C(1)	6774(3)	4680(3)	7547(2)	15(1)
C(2)	6921(3)	5495(3)	8508(3)	17(1)
C(3)	5851(3)	6874(3)	8149(3)	17(1)
C(4)	5056(3)	6881(3)	6983(3)	16(1)
C(5)	3884(3)	8095(3)	6284(3)	17(1)
C(6)	3091(3)	8200(3)	5130(2)	16(1)
C(7)	1936(3)	9512(3)	4436(3)	15(1)
C(8)	1470(3)	9150(3)	3369(3)	16(1)
C(9)	2372(3)	7623(3)	3420(3)	15(1)
C(10)	2310(3)	6808(3)	2464(3)	16(1)
C(11)	8000(3)	4932(3)	9678(3)	23(1)
C(12)	7424(4)	4249(3)	10844(3)	30(1)
C(13)	5552(3)	8150(3)	8808(3)	23(1)
C(14)	4230(3)	8485(3)	9643(3)	27(1)
C(15)	1444(3)	10992(3)	4786(3)	21(1)
C(16)	2493(3)	11713(3)	4330(3)	26(1)
C(17)	275(3)	10142(3)	2345(3)	21(1)
C(18)	841(4)	10823(3)	1183(3)	33(1)
C(19)	3933(3)	2946(3)	6928(3)	20(1)
C(20)	3006(3)	2419(3)	7611(3)	24(1)
C(21)	1490(3)	3233(3)	7445(3)	24(1)
C(22)	965(3)	4547(3)	6610(3)	26(1)
C(23)	1972(3)	4997(3)	5964(3)	20(1)

Table IV. Bond Lengths (Å) and Angles (deg) for $(py)_2Ni^{II}(OEPO^{\bullet})/(py)_2Ni^{II}(OEPO_2)$

Bond Lengths			
Ni–N(1)	2.063(2)	Ni–N(2)	2.062(2)
Ni–N(3)	2.226(2)	O(1)–C(10)	1.284(5)
O(1′)–C(5)	1.323(11)		
Bond Angles			
N(1)–Ni–N(2)	90.66(9)	N(1)–Ni–N(3)	90.91(8)
N(2)–Ni–N(3)	91.06(9)	N(1)–Ni–N(1a)	180
N(2a)–Ni–N(1)	89.34(9)	N(1)–Ni–N(3a)	89.09(8)
N(2)–Ni–N(3a)	88.94(9)	N(2)–Ni–N(2a)	180
N(3)–Ni–N(3a)	180		

(4) Å) seen in the paramagnetic ($S = 1$) complex $[(Im)_2Ni^{II}(TMPyP)](ClO_4)_4$.[18] The Ni–N(3) distance (2.226(2) Å) to the axial pyridine ligand is slightly longer than the Ni–N(imidazole) distance (2.160(4) Å) in $[(Im)_2Ni^{II}(TMPyP)](ClO_4)_4$.[18]

The macrocycle in this sample is nearly planar, as can be seen in the formal diagram in Figure 4.

Figure 7 shows a view of the solid-state packing of molecules in $(py)_2Ni^{II}(OEPO^{\bullet})/(py)_2Ni^{II}(OEPO_2)$. The presence of the two axial ligands serves to insulate the molecules from one another, and dimerization does not occur as it does in related complexes such as $\{[Ni^{II}(OEP^{\bullet})]ClO_4\}_2$[17] and $\{Ni^{II}_2(OEPO)_2\}$.[12]

Discussion

This work on nickel oxophlorin complexes complements the earlier work on analogous zinc complexes. While both nickel and zinc oxophlorin complexes readily dissolve in pyridine to form air-sensitive solutions, the zinc complex crystallized as five-coordinate (py)Zn^{II}(OEPOH··py) with a fully ordered structure, while the nickel complex crystallized as four-coordinate Ni^{II}(OEPOH) with disorder in the position of the meso hydroxy group. In the zinc complex, hydrogen bonding between the hydroxyl group and the pyridine is a major factor in producing an ordered system.

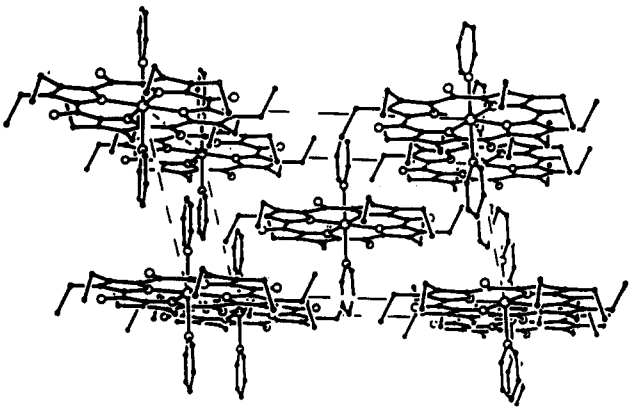

Figure 7. Solid-phase packing for $(py)_2Ni^{II}(OEPO^{\bullet})/(py)_2Ni^{II}(OEPO_2)$.

The ability of Ni^{II}(OEPOH) to form this nonplanar structure attests to the flexibility of the oxophlorin ring system. The distortion can be attributed to the small size of Ni^{II}, which is better accommodated by contraction of the macrocyclic core.

Ni^{II}(OEPOH) is readily oxidized to the brown radical $(py)_2$-Ni(OEPO$^{\bullet}$), which has been isolated in crystalline form. The characteristic electronic spectrum (trace B, Figure 1) and the observation of a free radical type EPR spectrum at $g = 2.006$ point to a ligand-based oxidation. However, further description of the electronic structure of this species is required. The structural work demonstrates that the nickel coordination geometry undergoes marked change upon oxidation. These changes are much more pronounced than the changes seen when (py)Zn-(OEPOH··py) is oxidized to (py)Zn^{II}(OEPO$^{\bullet}$).[7] The oxidation product, $(py)_2Ni^{II}(OEPO^{\bullet})$, is six-coordinate and has Ni–N(oxophlorin) distances that are indicative of a paramagnetic ($S = 1$) state for the nickel. This spin-state change results in population of the $d_{x^2-y^2}$ orbital and the observed expansion of the Ni–N distances. The close similarity of the nickel coordination in $(py)_2Ni(OEPO^{\bullet})$ and in paramagnetic ($S = 1$) $[(Im)_2Ni$-$(TMPyP)](ClO_4)_4$ strongly points to the presence of a metal ion with high-spin characteristics. Notice also that, in both of these complexes, the axial Ni–N bonds are long. This is indicative of population of the d_{z^2} orbital as well. However, the observed magnetic moment and the EPR spectrum suggest that the complex exists in an $S = {}^1/_2$ state. This can readily be accommodated if strong antiferromagnetic coupling exists between the oxophlorin radical and the high-spin nickel center. Such coupling could produce a complex with an effective $S = {}^1/_2$ ground state. However, prior work would have predicted ferromagnetic rather than antiferromagnetic coupling. The structural data indicate that the unpaired spins on nickel are orbitals of σ character. The oxophlorin radical has an unpaired electron in a π molecular orbital. Thus the spin-containing orbitals are orthogonal, and earlier work has anticipated ferromagnetic interactions when the magnetic orbitals are orthogonal.[18,19] However, slight ruffling of the macrocyclic core as seen in Figure 5 may be sufficient to cause orbital overlap and induce antiferromagnetic coupling.

This work shows that complexes of octaethyloxophlorin radical with some degree of axial ligation can resist dimerization. In contrast, the corresponding nickel(II) and zinc(II) octaethylporphyrin radical complexes form novel dimers, $[Zn(OEP^{\bullet})(OH_2)]_2$-$(ClO_4)_2$ and $[Ni(OEPO^{\bullet})]_2(ClO_4)_2$, which have strong cofacial interactions.[17,21] In part, the tendency of the nickel complex to resist dimerization can be attributed to the presence of two axial

(17) Song, H.; Orosz, R. D.; Reed, C. A.; Schedit, W. R. *Inorg. Chem.* **1990**, *29*, 4274.
(18) Kirner, J. F.; Garofalo, J.; Scheidt, W. R. *Inorg. Nucl. Chem. Lett.* **1975**, *11*, 107.
(19) Kahn, O.; Galy, J.; Journaux, Y.; Jaud, J.; Morgenstern-Badarau, I. *J. Am. Chem. Soc.* **1982**, *104*, 2165.
(20) Gans, P.; Buisson, G.; Dúee, E.; Marchon, J.-C.; Erler, B. S.; Scholz, W. F.; Reed, C. A. *J. Am. Chem. Soc.* **1986**, *108*, 1223.
(21) Song, H.; Reed, C. A.; Scheidt, W. R. *J. Am. Chem. Soc.* **1989**, *111*, 6867.

Table V. Crystal Structure Data

	Ni^{II}(OEPOH)	$(py)_2Ni^{II}(OEPO^{\bullet})$/ $(py)_2Ni^{II}(OEPO_2)$
formula	$C_{36}H_{43}N_4NiO$	$C_{46}H_{52.66}N_6NiO_{1.34}$
fw	606.5	769.75
space group	$I4_1/a$, tetragonal	$P\bar{1}$, triclinic
a, Å	14.780(9)	9.848(2)
b, Å		10.216(2)
c, Å	13.903(14)	10.492(2)
α, deg	90	80.34(3)
β, deg	90	89.82(3)
γ, deg	90	66.36(3)
V, Å^3	3037(4)	950.9(3)
Z	4	1
T, K	130	123
λ, Å	0.710 69 (MoKα)	1.541 78 (CuKα)
μ, mm^{-1}	0.675	1.091
d_{calc}, Mg/m^3	1.326	1.344
transm factors	0.87–0.94	0.93–0.96
R^a	0.057	0.036
$R_w^{b,c}$	0.077[b]	0.068[c]

[a] $R = \sum||F_o| - |F_c||/\sum|F_o|$. [b] $R_w = [\sum[w(F_o - F_c)^2]/\sum[w(F_o^2)]]^{1/2}$. [c] $R_{w2} = [\sum[w(F_o^2 - F_c^2)^2]/\sum[w(F_o^2)^2]]^{1/2}$.

ligands. The effective delocalization available to the oxophlorin complex also assists in stabilizing the radical just as hydroxylation of benzene produces the much more easily oxidized phenol. Removal of the axial ligands, however, does lead to dimerization as shown in eq 1.[12] Unlike the case with the porphyrin radical, dimerization of $Ni^{II}(OEPO^{\bullet})$ results in the formation of a discreet carbon–carbon bond.

Both of the structures reported here suffer from significant disorder in the position of the meso oxygen substituents. This sort of disorder is common in core-modified porphyrins as we have pointed out previously.[7] It occurs largely because the positioning of the small meso hydroxyl or keto group does little to alter the external shape of the macrocycle. The fact that $(py)_2Ni^{II}(OEPO^{\bullet})$, $(py)_2Ni^{II}$(*trans*-$OEPO_2$), and $(py)_2Ni^{II}$(*cis*-$OEPO_2$) all crystallize in the same way indicates a poor degree of molecular recognition during crystallization. Generally, the act of crystallization is accompanied by a remarkable ability of the growing crystal to recognize like molecules. In this case, however, the spatial volume of the oxygen atoms at the meso sites is effectively masked by the neighboring ethyl groups. The effect of the dipolar nature of these molecules in governing their orientation must also be insufficient to compensate for the similarity in their external shapes.

While the slow process of crystallization of $(py)_2Ni^{II}(OEPO^{\bullet})$ led to the formation of the mixed crystals of $(py)_2Ni^{II}(OEPO^{\bullet})$/ $(py)_2Ni^{II}(OEPO_2)$, solid samples of $(py)_2Ni^{II}(OEPO^{\bullet})$ that are essentially free of the dioxo complexes can be obtained by the oxidation of Ni^{II}(OEPOH) by diiodine in pyridine or by exposure of Ni^{II}(OEPOH) in pyridine to dioxygen for a few hours. Notice that the sample used to obtain the electronic spectrum shown in trace B of Figure 1 was free of contamination by the dioxo complexes, which show broad bands at *ca.* 600 nm.[13] It also has been briefly noted that the metal-free octaethyloxophlorin radical is converted by dioxygen into octaethyldioxoporphodimethene.[6]

Experimental Section

Preparation of Compounds. Octaethyloxophlorin (H_2OEPOH) was prepared by a known route.[22]

Ni^{II}(OEPOH). Octaethyloxophlorin (20 mg, 0.036 mmol) was added to a boiling solution of 45 mg (0.091 mmol) of nickel(II) acetate tetrahydrate and 12 mg (0.182 mmol) of sodium acetate in 20 mL of glacial acetic acid. The solution was heated under reflux for 10 min. The hot, red solution was filtered, and the filtrate was cooled. The red crystalline product was collected by filtration, washed with methanol, and vacuum-dried (yield 16.3 mg, 74%). Infrared (Nujol mull) (cm^{-1}): 3534 s, 1716 w, 1673 w, 1632 m, 1602 m, 1584 m, 1537 w, 1506 m, 1409 m, 1314 s, 1271 s, 1227 s, 1208 s, 1168 m, 1155 w, 1147 m, 1127 m, 1110 w, 1100 w, 1056 s, 1017 s, 1005 m, 991 m, 957 s, 925 w, 888 m, 835 m, 830 s, 793 m, 760 w, 749 m, 734 w, 726 w, 717 m, 708 w, 701 m, 685 m.

$(py)_2Ni^{II}(OEPO^{\bullet})$. A 50-mg (0.082-mmol) sample of Ni^{II}(OEPOH) was dissolved in 10 mL of pyridine, and 2 mL of a 1.97×10^{-2} M solution of diiodine in pyridine was added. The red solution turned brown with a green tinge. After the solution was stirred for 15 min, the solvent was removed under vacuum. The solid was dissolved in a minimum volume of pyridine and reprecipitated by the addition of methanol to give deep green crystals (yield 30.0 mg, 48%). Infrared (Nujol mull) (cm^{-1}): 1626 m, 1599 w, 1582 m, 1579 w, 1525 m, 1345 m, 1271 m, 1260 w, 1226 w, 1215 w, 1150 w, 1125 w, 1092 m, 1060 w, 1011 m, 975 w, 953 m, 905 w, 883 m, 850 w, 789 m, 749 m, 725 w, 713 w, 695 m, 629 m.

Conversion of Ni^{II}(OEPOH) into Ni^{II}(*trans*-$OEPO_2$) and Ni^{II}(*cis*-$OEPO_2$). A 15.7-mg (0.0257-mmol) sample of Ni^{II}(OEPOH) was dissolved in 10 mL of pyridine, and the solution was stored under an atmosphere of dioxygen for 3 days. The sample was then evaporated to dryness, and the residue was redissolved in a minimum of dichloromethane. This solution was subjected to chromatography on silica gel. The orange band that eluted first (with dichloromethane as eluent) was collected and evaporated to yield 12.9 mg (80%) of a mixture of Ni^{II}(*trans*-$OEPO_2$) and Ni^{II}(*cis*-$OEPO_2$). These complexes were identified by a spectral comparison with authentic samples.[13] Analysis by ^{1}H NMR spectroscopy revealed the presence of Ni^{II}(*trans*-$OEPO_2$) and Ni^{II}(*cis*-$OEPO_2$) in a 2:1 ratio. The yellow-green band, which was the second to elute with chloroform as solvent, was also collected and evaporated to yield 2.2 mg (14%) of Ni^{II}(OEPOH).

X-ray Data Collection. Ni^{II}(OEPOH). A dark red square pyramid was obtained by diffusion of dioxygen-free methanol into a dioxygen free pyridine solution of the complex. During crystallization, the solution remained red. A suitable crystal was coated with a light hydrocarbon oil and mounted in the 123 K dinitrogen stream of a Siemens R3m/V diffractometer equipped with a locally modified low-temperature apparatus. A tetragonal unit cell was obtained by indexing reflections from a rotation photograph and verified by examination of axial photographs. Two check reflections showed only random (<2%) variation in intensity during data collection. The data were corrected for Lorentz and polarization effects. Crystal data are collected in Table V.

$(py)_2Ni^{II}(OEPO^{\bullet})$/$(py)_2Ni^{II}(OEPO_2)$. Red parallelepipeds were obtained by diffusion of methanol into a brown pyridine solution of $(py)_2Ni^{II}(OEPO^{\bullet})$ without precautions to exclude dioxygen. A suitable crystal was coated with a light hydrocarbon oil and mounted in the 130 K dinitrogen stream of a Siemens P4RA diffractometer that was equipped with a locally modified, low-temperature apparatus. Data collection and handling proceeded as described above, with relevant information given in Table V.

Solution and Structure Refinement. Calculations were performed on a DEC VAXstation 3200 with SHELXTL Plus v. 4.00 and SHELXL-93. Scattering factors and corrections for anomalous dispersion were taken from a standard source.[23] The solution for each compound was determined from the Patterson function and subsequent cycles of least-squares refinement and calculation of difference Fourier maps. For Ni^{II}(OEPOH), hydrogen atoms were included using a riding model with fixed isotropic U. For $(py)_2Ni^{II}(OEPO^{\bullet})$/$(py)_2Ni^{II}(OEPO_2)$, hydrogen atoms were modeled with an isotropic U that rode as $1.2U_{eq}$ of the adjacent, bonded carbon atom. Absorption corrections were applied.[24] All non-hydrogen atoms were refined with anisotropic thermal parameters. For Ni^{II}(OEPOH), the largest difference peak was 0.35 e Å^{-3} and the meso hydroxyl group was disordered over four equally populated sites. For $(py)_2Ni^{II}(OEPO^{\bullet})$/$(py)_2Ni^{II}(OEPO_2)$, the meso oxygen was also disordered. Attempts to refine a model in which a single oxygen atom was disordered over the four meso sites gave unreasonably small thermal

(22) Barnett, G. H.; Hudson, M. F.; McCombie, S. W.; Smith, K. M. *J. Chem. Soc., Perkin Trans. 1* **1973**, 691.

(23) *International Tables for X-ray Crystallography*; Kynoch Press: Birmingham, England, 1974; Vol. 4.

(24) XABS (correction for Ni^{II}(OEPOH) obtains an empirical absorption tensor from an expression relating F_o and F_c: Moezzi, B. Ph.D. Thesis, University of California, Davis, 1987. XABS2 (correction for $(py)_2Ni^{II}(OEPO^{\bullet})$/$(py)_2Ni^{II}(OEPO_2)$) (S. Parkin, 1992) calculates 24 coefficients from a least-squares fit of $1/A$ vs $\sin^2\theta$ to a cubic equation in $\sin^2\theta$ by minimization of F_o^2 and F_c^2 differences.

parameters. At that stage, further refinement of the oxygen atom with the allowance for anisotropic motion led to unreasonable behavior of that atom. Consequently, the oxygen thermal parameters were fixed at value (0.0180 Å^2) that was just slightly larger than the average thermal parameter for the carbons of the porphyrin core. After refinement of this model, the occupancy of the O(1) site was 0.446 while that at the O(1′) site (adjacent to C(5)) was 0.231. These occupancy factors were then fixed, and the thermal parameters for these atoms, along with all others, were allowed to refine anisotropically. The largest peak in the final difference map was 0.19 e Å^{-3}, and the largest hole was −0.35 e Å^{-3}.

Instrumentation. ^{1}H NMR spectra were recorded on a General Electric QE 300 Fourier transform spectrometer. Electronic spectra were obtained through the use of a Hitachi U-2000 spectrophotometer.

Acknowledgment. We thank the NIH (Grant GM26226) for financial support.

Supplementary Material Available: Tables of bond distances, bond angles, anisotropic thermal parameters, hydrogen atom coordinates, and crystal data for Ni^{II}(OEPOH) and $(py)_2Ni^{II}$(OEPO$^{\bullet}$)/$(py)_2Ni^{II}$($OEPO_2$) (11 pages). Ordering information is given on any current masthead page.